

Designing highly efficient Rh/CPOL-bp&PPh₃ heterogenous catalysts for hydroformylation of internal and terminal olefins

Cunyao Li,^{ac} Kai Xiong,^d Li Yan,^{*b} Miao Jiang^{ac}, Xiangen Song^a, Tao Wang^{ac}, Xingkun Chen^{ac}, Zhuangping Zhan^d and Yunjie Ding^{*ab}

^aDalian National Laboratory for Clean Energy, Dalian, 116023, P. R. China

^bState Key Laboratory of catalysis, Dalian Institute of Chemical Physics, Chinese Academy of Sciences, Dalian, 116023, P. R. China

^cUniversity of Chinese Academy of Sciences, Beijing 100039, P. R. China

^dDepartment of Chemistry, College of Chemistry and Chemical Engineering, Xiamen University, Xiamen 361005, P. R. China

1. SUPPORTING FIGURES	- 3 -
2. SUPPORTING TABLES	- 15 -
3. NMR CHARACTERIZATIONS OF COMPOUNDS IN SCHEME 1	- 16 -

1. Supporting Figures

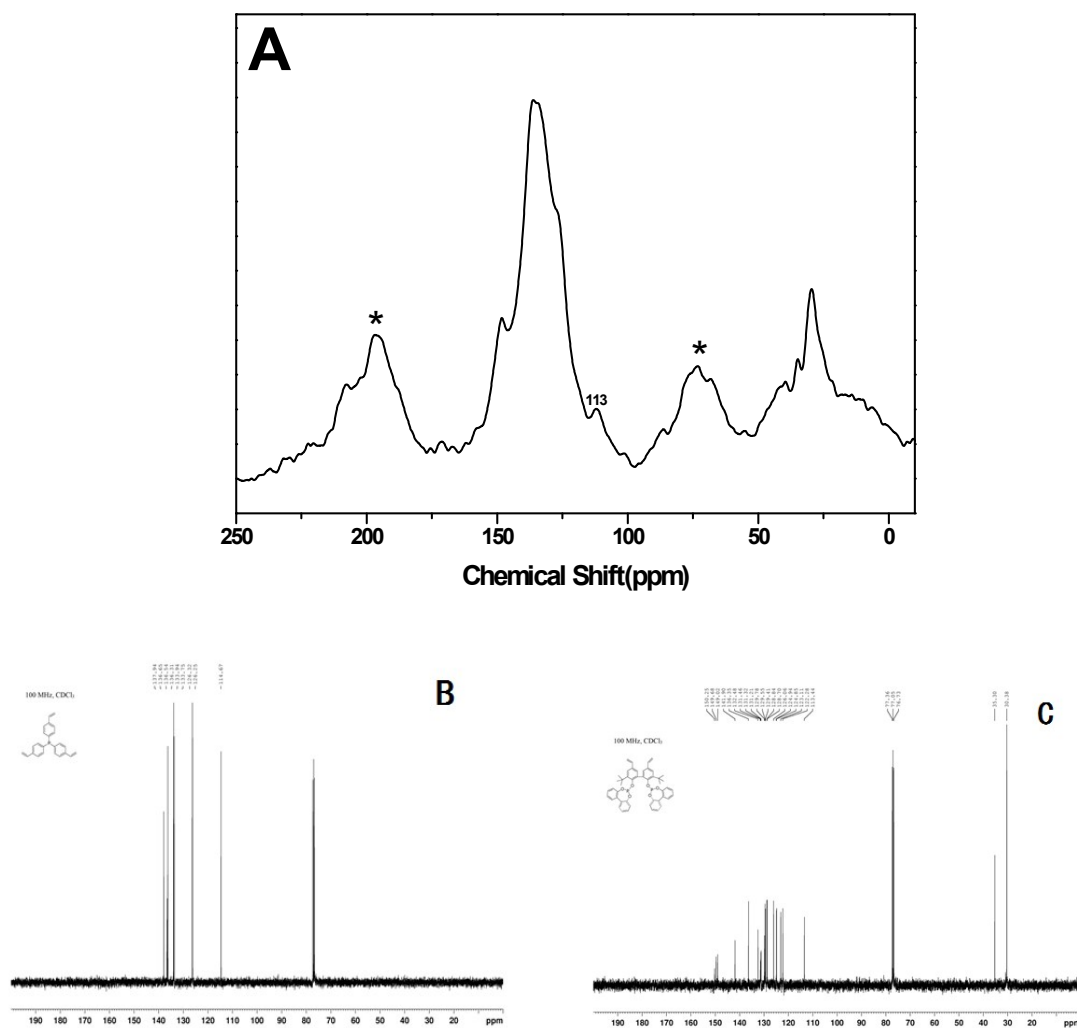


Figure S1. (A) ^{13}C MAS NMR spectrum of CPOL-bp&PPh₃, (B) ^{13}C NMR spectrum of tris(4-vinylphenyl)phosphane and (C) ^{13}C NMR spectrum of vinyl biphenos.

The peaks at 113 ppm in CPOL-bp&PPh₃, which can be assigned to unpolymerized vinyl groups, is quite small compared with the corresponding monomers (B, C), indicating that CPOL-bp&PPh₃ has high degree of polymerization. The peaks at * are side bands.

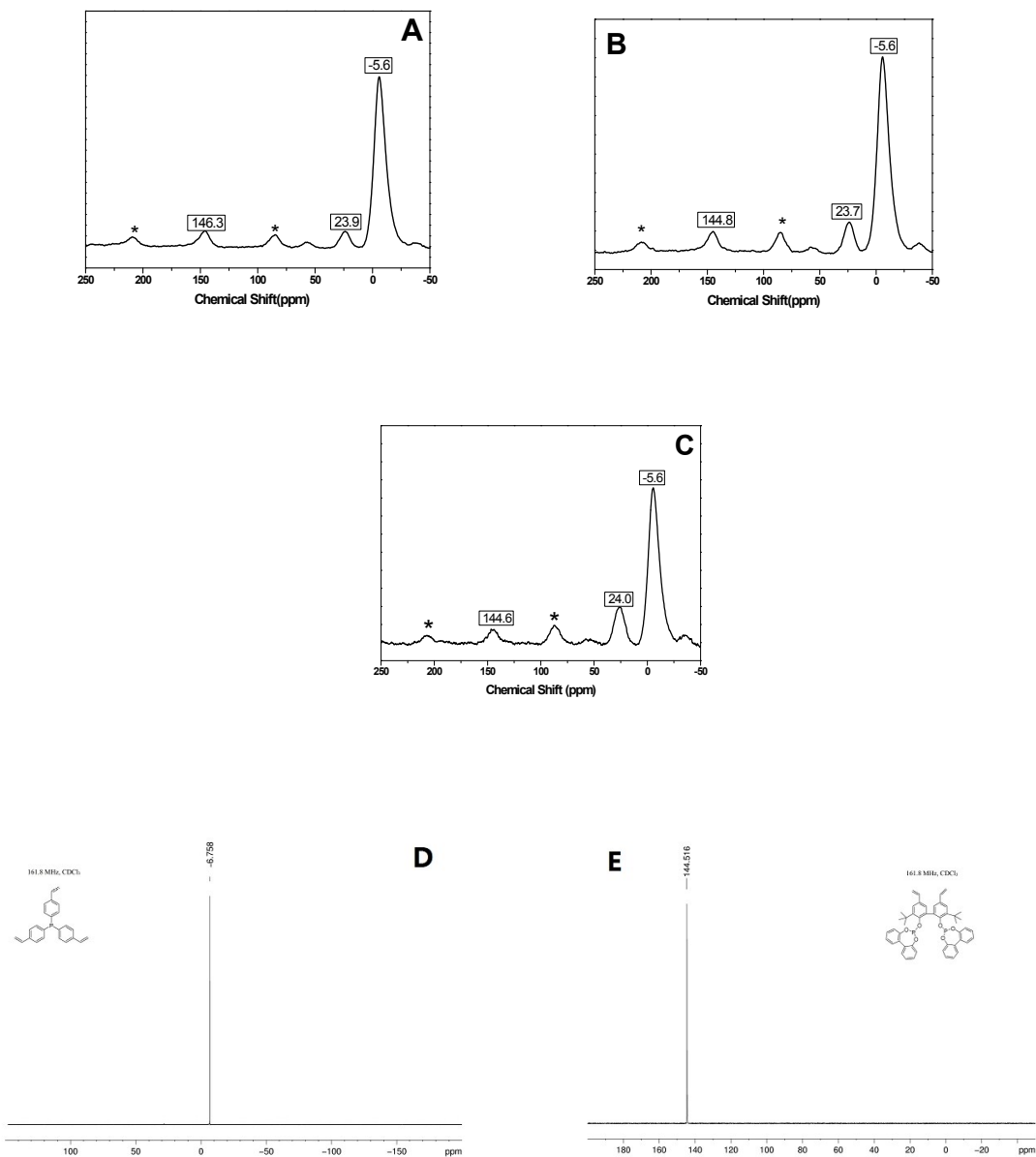


Figure S2. ^{31}P MAS NMR spectra of (A) CPOL-bp&PPh₃, (B) 0.14 % wt Rh/CPOL-bp&PPh₃ and (C) 2.0 % wt Rh/CPOL-bp&PPh₃, ^{31}P NMR spectra of (D) tris(4-vinylphenyl)phosphane and (E) vinyl biphenos.

The peaks at * are side bands. The ^{31}P MAS NMR spectrum of fresh CPOL-bp&PPh₃ exhibits an additional small peak at 23.9 ppm corresponding to an oxidation state of phosphorus (P=O), which indicates that slight oxidation of P atom took place during the polymerization. Remarkably, the ^{31}P MAS NMR spectrum of fresh 0.14 % wt Rh/CPOL-bp&PPh₃ shows that the peak at 23.7 ppm could be assigned to both oxidation state of phosphorus (P=O) and those PPh₃ coordinated with Rh as well. 2.0 % wt Rh/CPOL-bp&PPh₃ shows higher peak at 24.0 ppm than 0.14 % wt Rh/CPOL-bp&PPh₃, indicating more PPh₃ units are coordinated with Rh. Besides, compared with the peak at 146.3 ppm in CPOL-bp&PPh₃, 0.14% wt Rh/CPOL-bp&PPh₃ gives relatively low-field peak at 144.8 ppm, 2.0 % wt Rh/CPOL-bp&PPh₃ gives relatively low-field peak at 144.6 ppm. The low-field shift can be ascribed to the biphenos units coordinated with Rh.

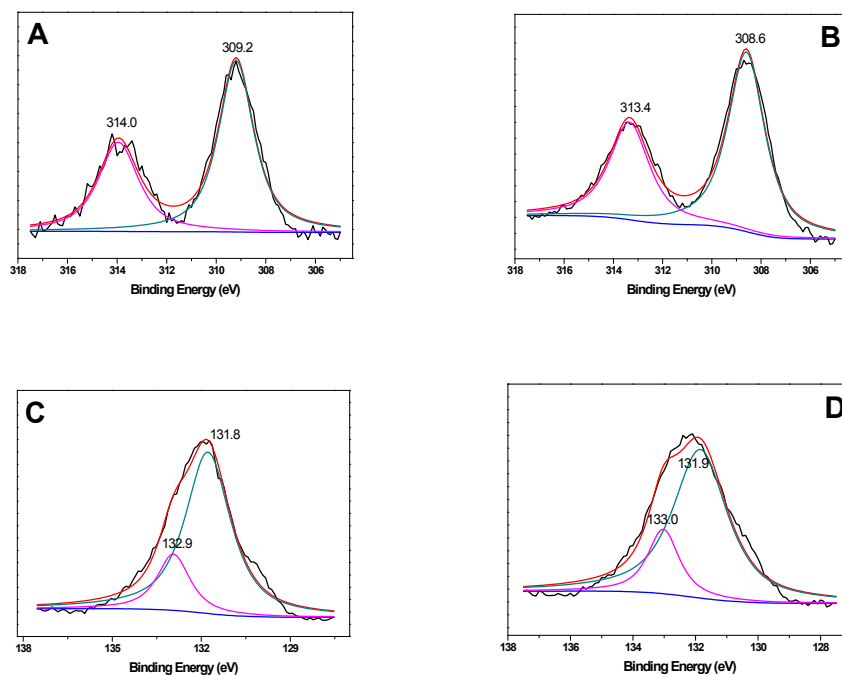


Figure S3. (A) Rh3d XPS spectra of Rh(CO)₂(acac), (B) Rh3d XPS spectra of 0.14% Rh/CPOL-bp&PPh₃, (C) P2p XPS spectra of CPOL-bp&PPh₃, (E) P2p XPS spectra of 0.14% Rh/CPOL-bp&PPh₃.

XPS of Rh(CO)₂(acac) shows the binding energies of Rh3d_{3/2} and Rh3d_{5/2} at 314.0 eV and 309.2 eV respectively. In 0.14% Rh/CPOL-bp&PPh₃ catalyst, the binding energies of Rh3d_{3/2} and Rh3d_{5/2} decrease to 313.4 eV and 308.6 eV, showing the successful coordination of Rh(CO)₂acac with CPOL-bp&PPh₃ carrier. Interestingly, compared with XPS spectra of P2p in CPOL-bp&PPh₃ (two kinds of P species: PPh₃ units at 131.8 eV, biphphos units at 132.9 eV), 0.14% Rh/CPOL-bp&PPh₃ give relatively higher binding energy (131.9 eV, 133.0 eV), indicating the successful coordination of Rh with two kinds of P species in the polymer skeleton.

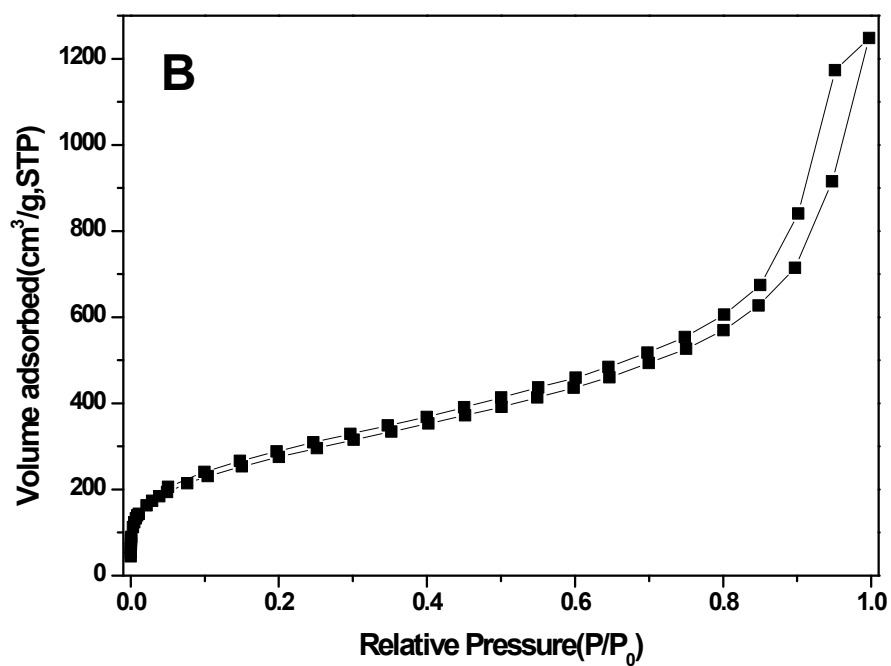
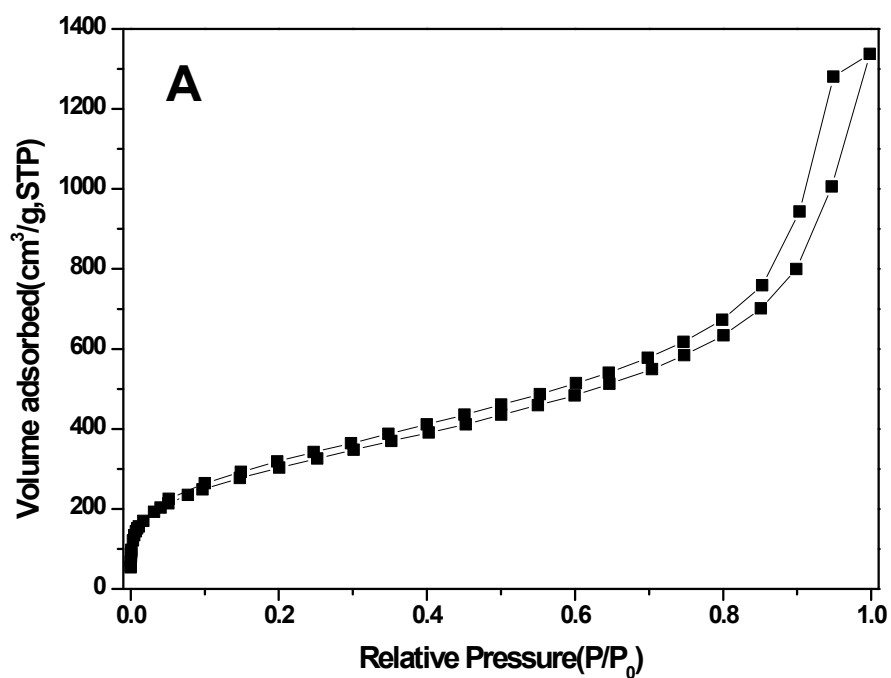


Figure S4. Nitrogen sorption isotherms of (A) CPOL-bp&PPh₃ and (B) Rh/CPOL-bp&PPh₃.

Figure S4 indicates that N₂ sorption isotherm of both CPOL-bp&PPh₃ and Rh/CPOL-bp&PPh₃ give the curve of type-I plus type-IV, showing that the two samples possess both micropores and mesoporous.

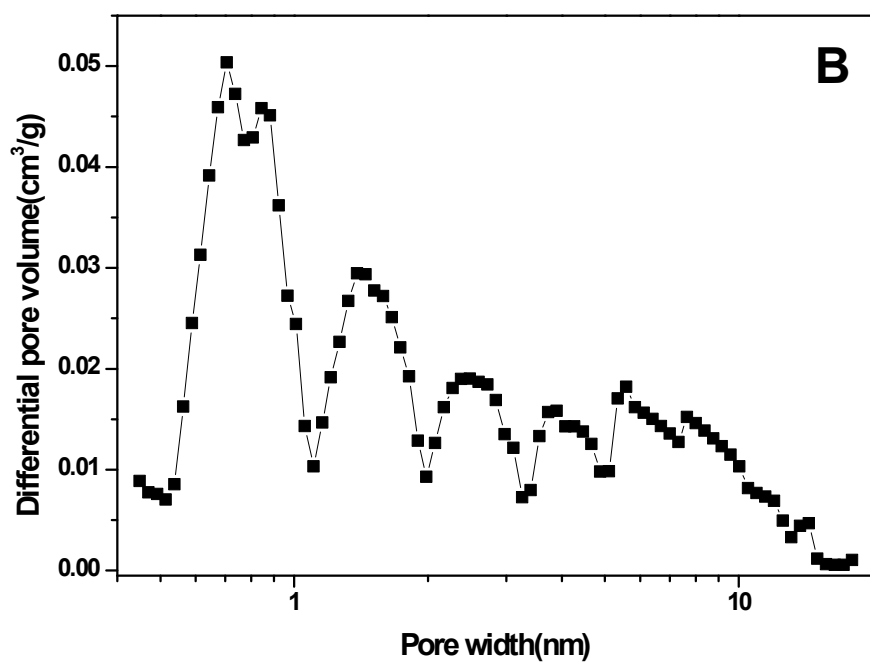
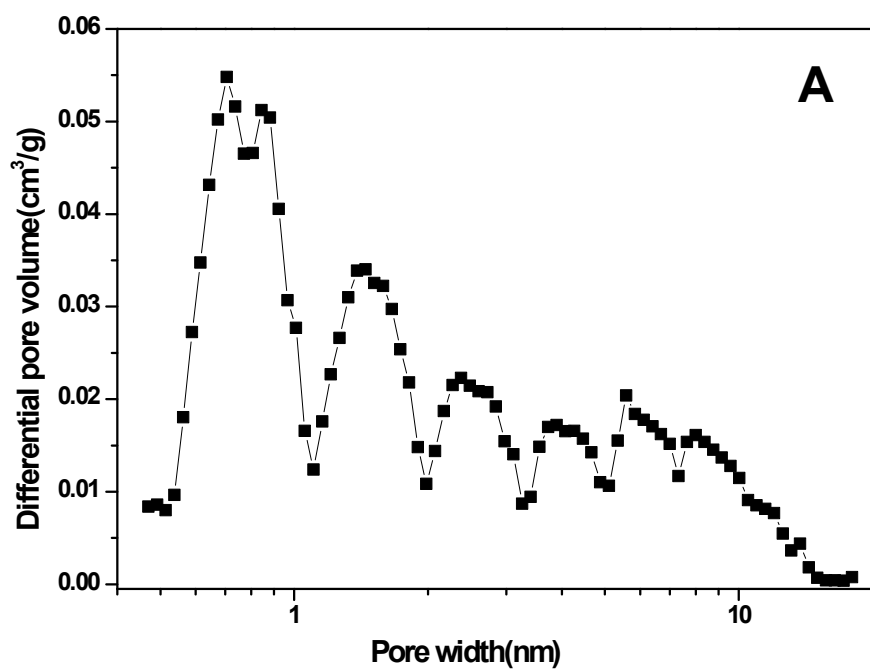


Figure S5. Pore size distribution of (A) CPOL-bp&PPh₃ and (B) Rh/CPOL-bp&PPh₃.

Pore size distribution is calculated from non-local density functional theory (NLDFT). Figure S5 indicates that both CPOL-bp&PPh₃ and Rh/CPOL-bp&PPh₃ possess hierarchical porosity.

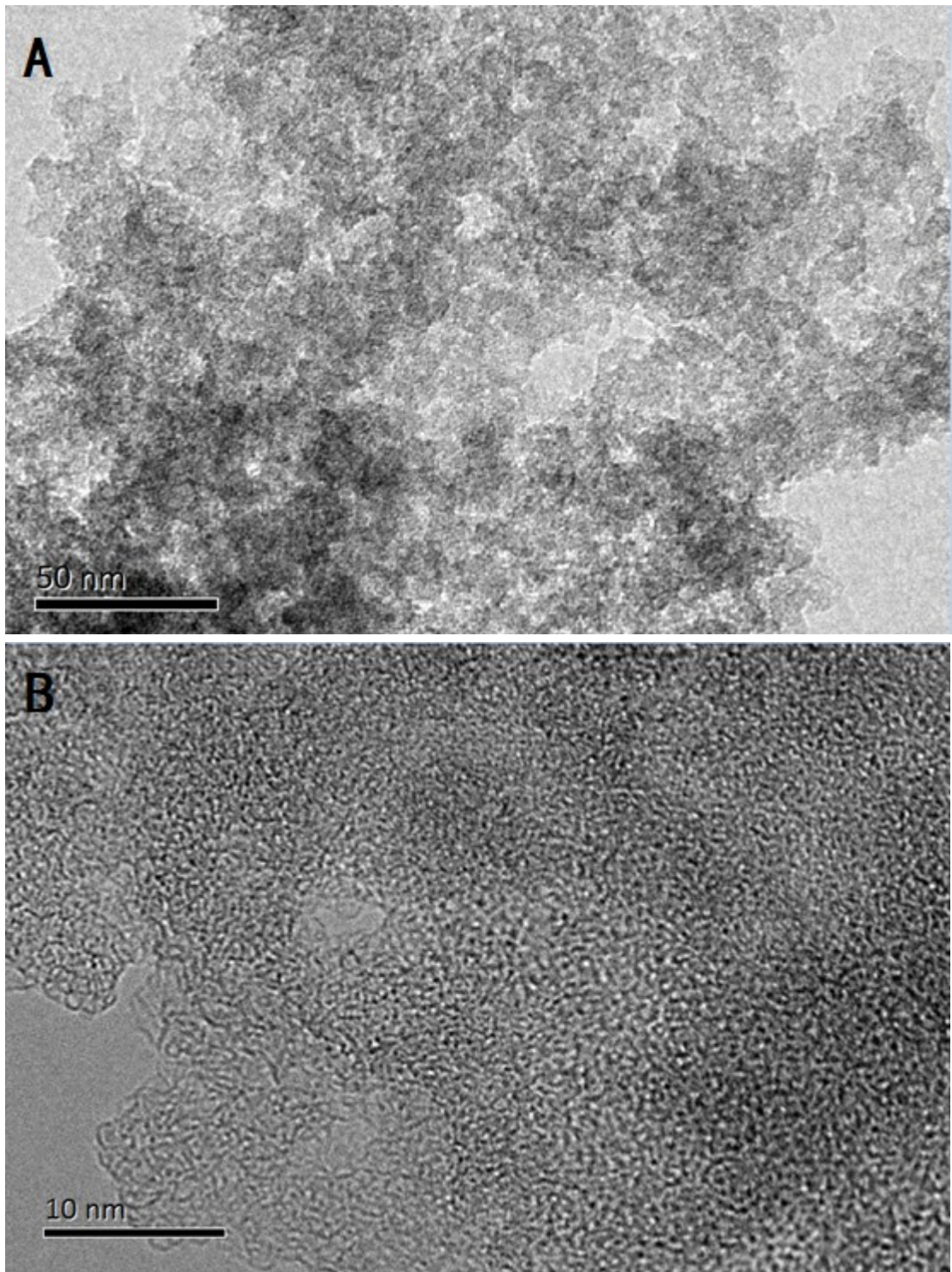


Figure S6. TEM images of CPOL-bp&PPh₃.

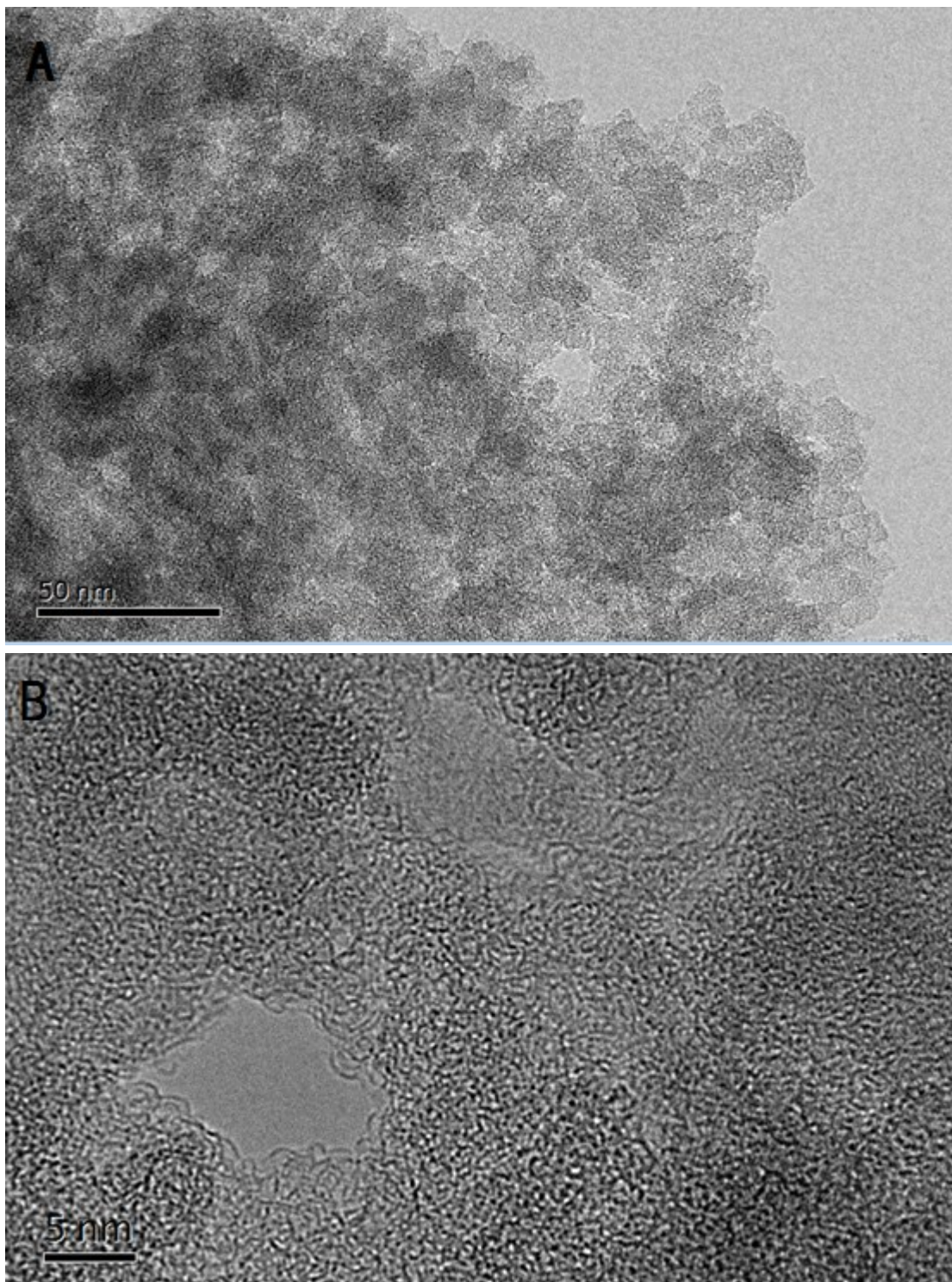


Figure S7. TEM images of Rh/CPOL-bp&PPh₃.

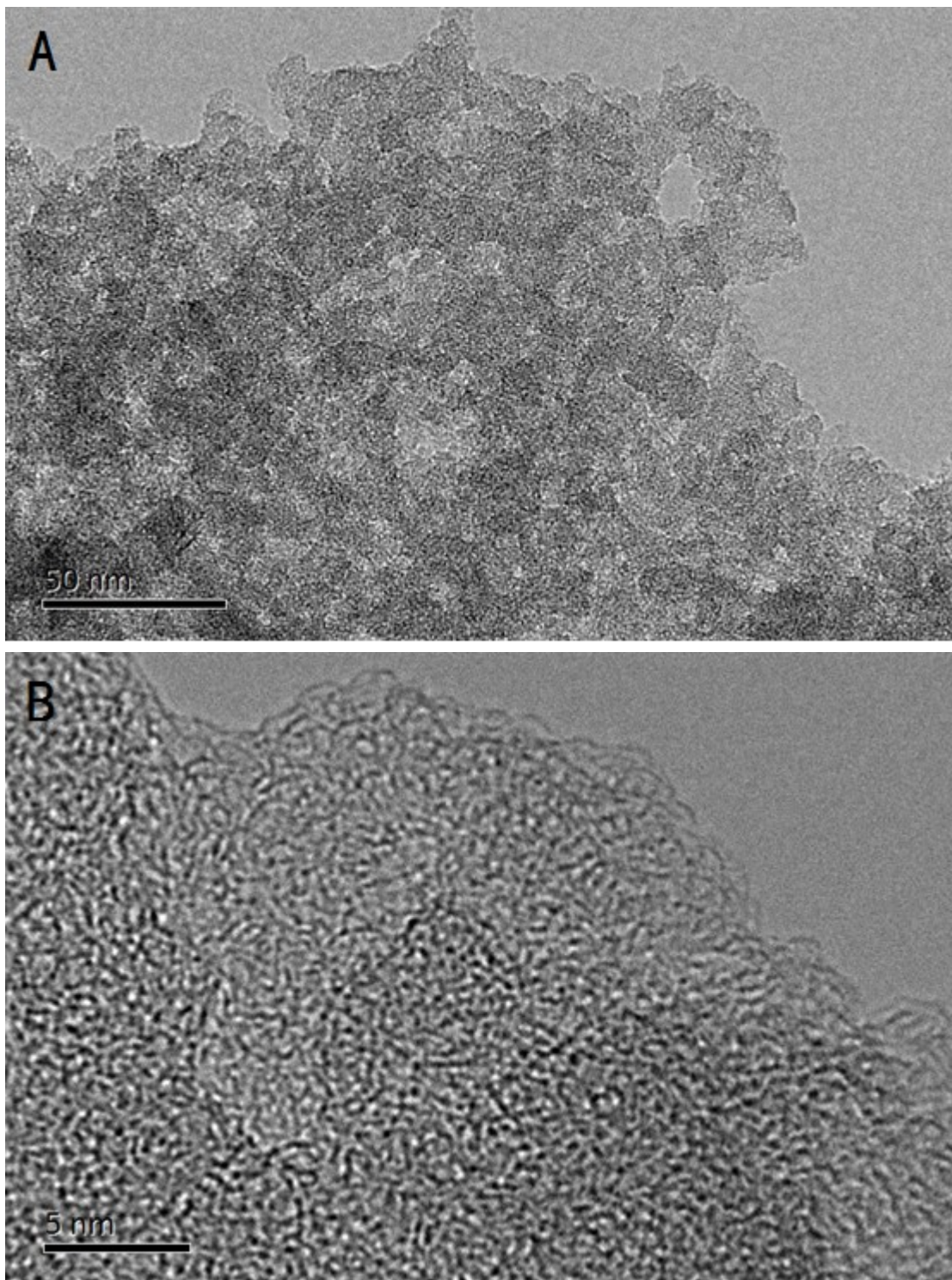
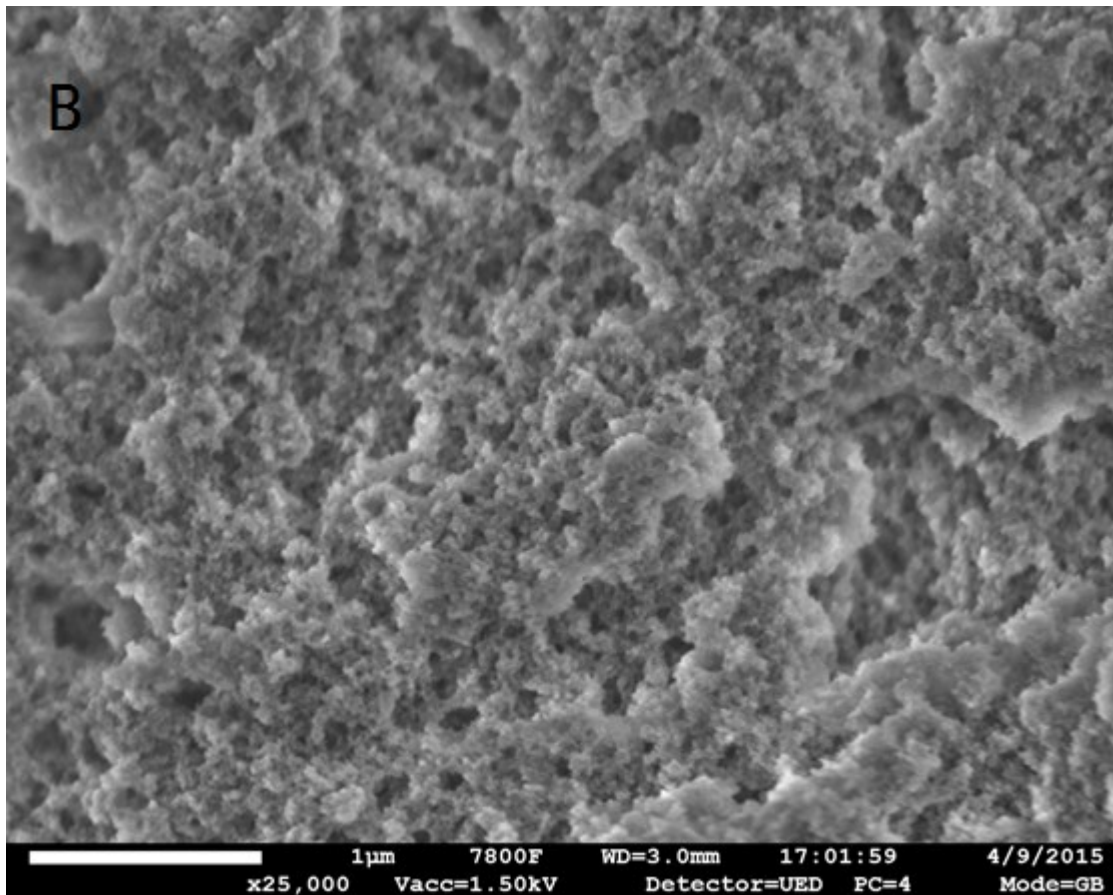
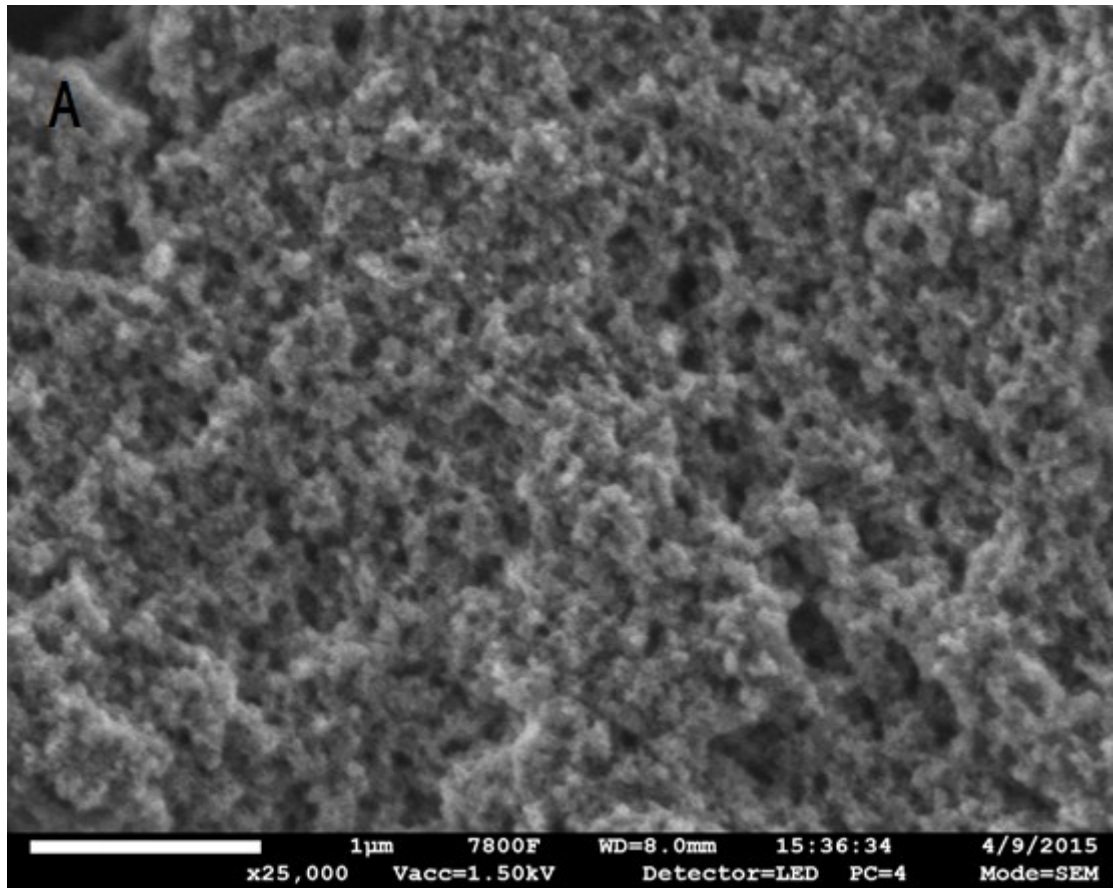


Figure S8. TEM images of Rh/CPOL-bp&PPh₃ after 6 runs.



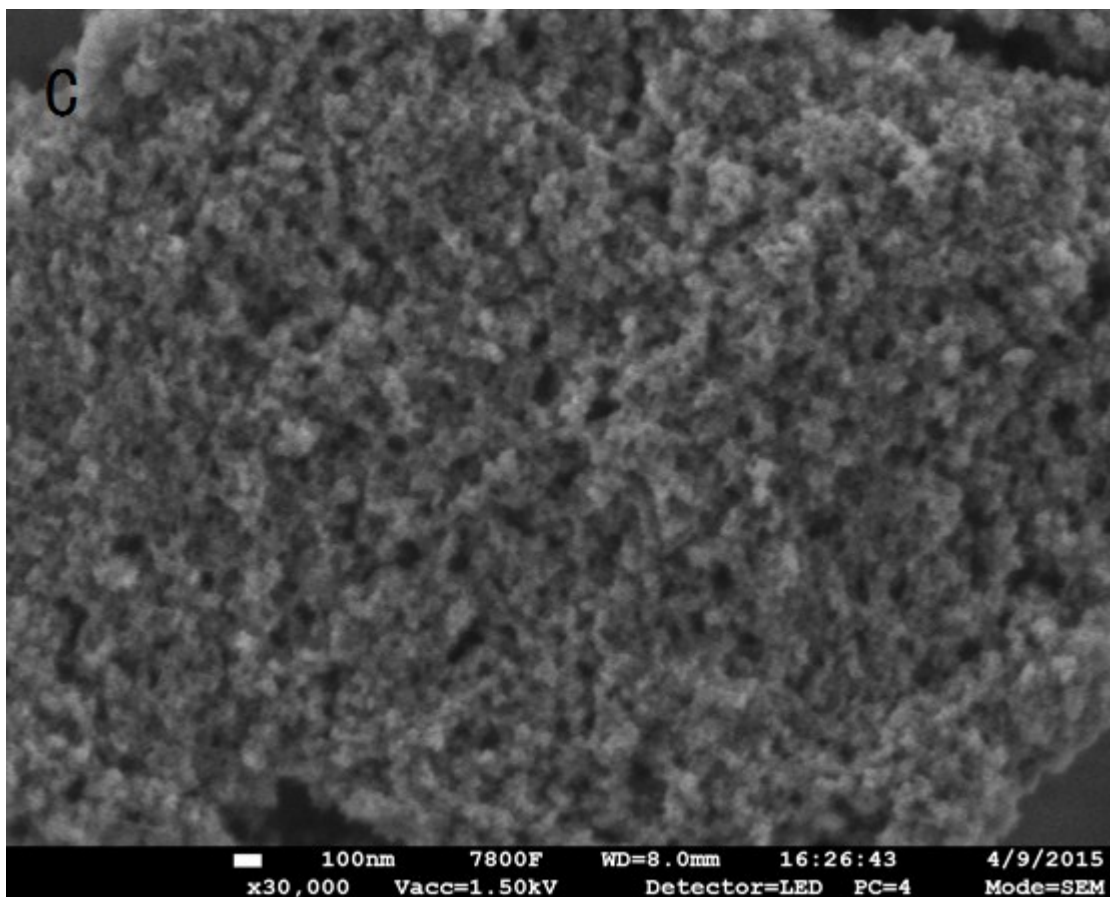
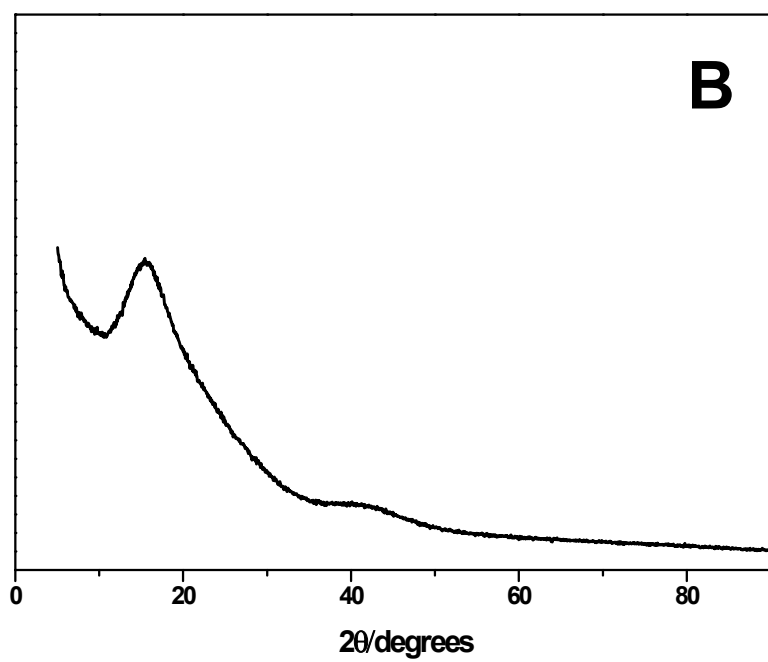
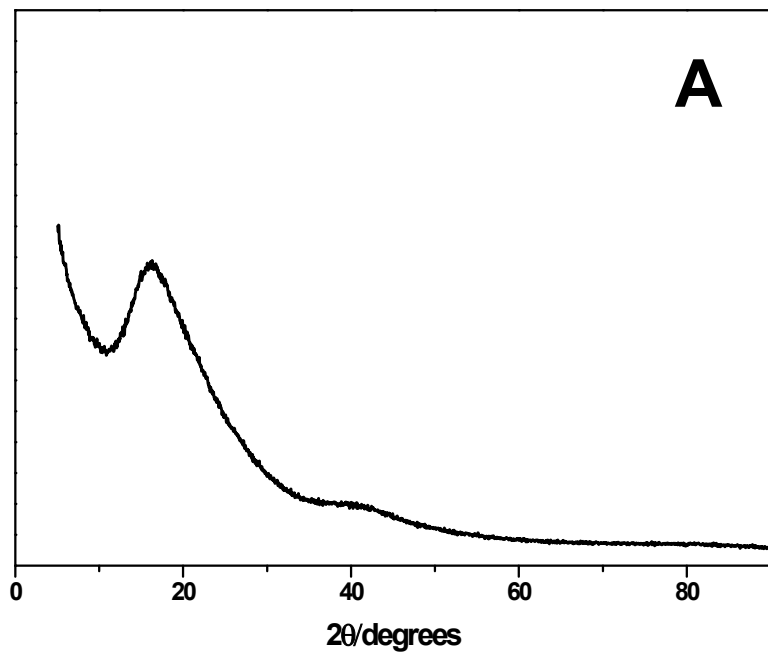


Figure S9. SEM images of (A) CPOL-bp&PPh₃, (B) Rh/CPOL-bp&PPh₃ and (C) Rh/CPOL-bp&PPh₃ after 6 runs.

Figure S9 shows that the all the samples have hierarchical porosity.



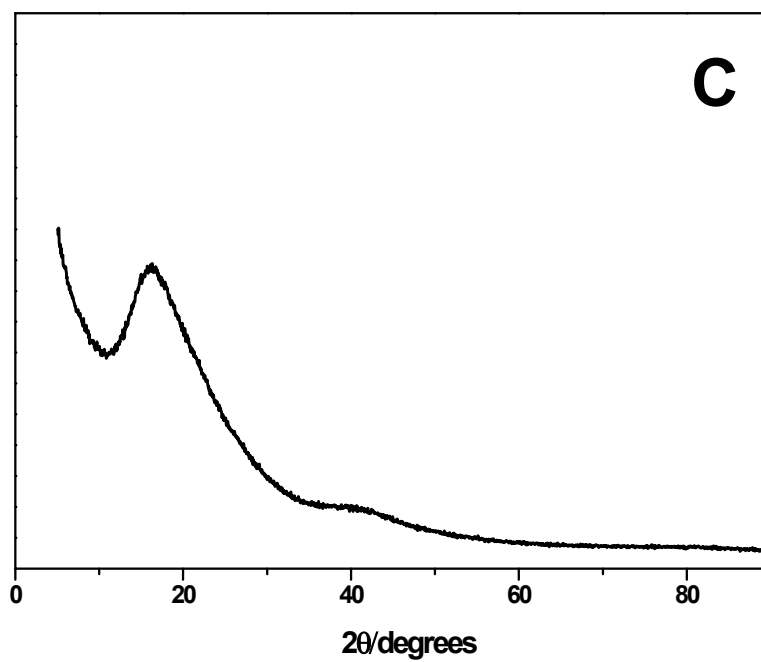


Figure S10. XRD of (A) CPOL-bp&PPh₃, (B) Rh/CPOL-bp&PPh₃ and (C) Rh/CPOL-bp&PPh₃ after 6 runs.

XRD also show that all three samples are amorphous.

2. Supporting Tables

Table S1. Rh concentration of fresh and spend catalysts

Sample	Rh content(wt.%) ^a
Rh/CPOL-bp&PPh ₃ (fresh sample)	0.1385%
Rh/CPOL-bp&PPh ₃ (spend sample, 6 runs)	0.1340%

^a The lowest detectable limit of ICP-OES is 10⁻⁶, "85" and "40" in Rh content are untrusted data.

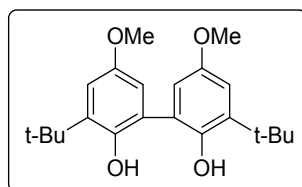
3. NMR characterizations of compounds in Scheme 1

Analytical data for compounds 1-7 and A, B

^1H and ^{13}C spectra were recorded on a 500 MHz spectrometer. Chemical shifts were reported in ppm. ^1H NMR spectra were referenced to TMS in CDCl_3 (0 ppm) or d_6 -DMSO (0 ppm), and ^{13}C -NMR spectra were referenced to CDCl_3 (77.0 ppm) or d_6 -DMSO (39.5 ppm). All ^{13}C -NMR spectra were measured with complete proton decoupling except compound (A). Peak multiplicities were designated by the following abbreviations: s, singlet; d, doublet; t, triplet; m, multiplet; brs, broad singlet and J, coupling constant in Hz.

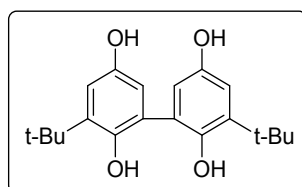
Mass spectroscopy were recorded on a Esquire 3000 Plus mass spectrometer. We were grateful to the assistance of the Department of Chemistry, Xiamen University in obtaining the MS data.

5,5'-dimethoxy-3,3'-di-*tert*-butylbiphenyl-2,2'-diol (1)



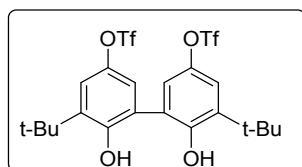
off-white powder, m.p. 220 °C; ^1H NMR (400 MHz, CDCl_3) δ 1.43 (s, 9H), 3.77 (s, 3H), 5.04 (s, 1H), 6.62 (d, 1H, $J = 3.0$ Hz), 6.96 (d, 1H, $J = 3.0$ Hz); ^{13}C NMR (100 MHz, CDCl_3) δ 29.5, 35.2, 55.7, 111.8, 115.3, 123.3, 138.9, 145.9, 153.2.

3,3'-di-*tert*-butylbiphenyl-2,2',5,5'-tetraol (2)



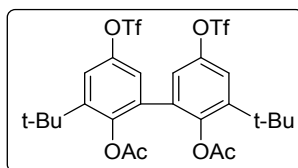
white chalky solid, m.p. 222 °C; ^1H NMR (400 MHz, $\text{DMSO}-d_6$) δ 1.36 (s, 9H), 6.49 (d, 1H, $J = 2.9$ Hz), 6.68 (d, 1H, $J = 2.9$ Hz), 8.39 (s, 1H), 8.86 (s, 1H); ^{13}C NMR (100 MHz, $\text{DMSO}-d_6$) δ 30.3, 35.1, 113.6, 115.4, 131.6, 140.8, 144.1, 151.4.

5,5'-di-*tert*-butyl-6,6'-dihydroxybiphenyl-3,3'-diyl bis(trifluoromethanesulfonate) (3)



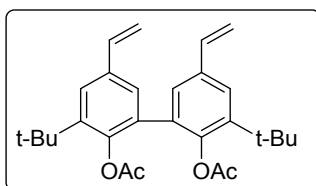
Gummy liquid; ^1H NMR (500 MHz, CDCl_3) δ 1.45 (s, 9H), 5.44 (s, 1H), 7.04 (d, 1H, $J = 3.1$ Hz), 7.30 (d, 1H, $J = 3.1$ Hz); ^{13}C NMR (125 MHz, CDCl_3) δ 29.2, 35.5, 118.8 (q, $J = 320.0$ Hz), 121.2, 121.8, 122.5, 140.6, 142.9, 151.7.

6,6'-diacetate-5,5'-di-*tert*-butylbiphenyl-3,3'-diyl bis(trifluoromethanesulfonate) (4)



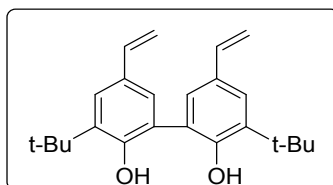
a white solid, m.p. 109 °C; $^1\text{H NMR}$ (400 MHz, CDCl_3) δ 1.38 (s, 9H), 1.85 (s, 3H), 7.06 (d, 1H, $J = 2.9$ Hz), 7.36 (d, 1H, $J = 3.1$ Hz); $^{13}\text{C NMR}$ (100 MHz, CDCl_3) δ 20.4, 29.9, 35.2, 118.8 (q, $J = 321.0$ Hz), 120.9, 122.4, 133.6, 144.9, 146.4, 146.6, 167.9.

3,3'-di-*tert*-butyl-5,5'-divinylbiphenyl-2,2'-diyl diacetate (5)



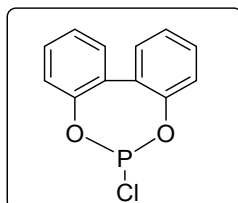
a white solid, m.p. 118 °C; $^1\text{H NMR}$ (500 MHz, CDCl_3) δ 1.38 (s, 9H), 1.84 (s, 3H), 5.22 (d, 1H, $J = 11.2$ Hz), 5.70 (dd, 1H, $J_1 = 17.6$ Hz, $J_2 = 0.6$ Hz), 6.70 (dd, 1H, $J_1 = 17.6$ Hz, $J_2 = 10.9$ Hz), 7.24 (d, 1H, $J = 1.9$ Hz), 7.41 (d, 1H, $J = 2.1$ Hz); $^{13}\text{C NMR}$ (100 MHz, CDCl_3) δ 20.8, 30.4, 34.7, 114.0, 125.0, 127.9, 133.4, 135.4, 136.4, 141.3, 146.4, 168.6.

3,3'-di-*tert*-butyl-5,5'-divinylbiphenyl-2,2'-diol (6)



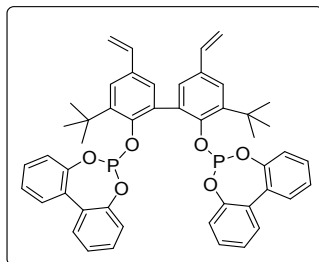
a white solid, m.p. 55 °C; $^1\text{H NMR}$ (500 MHz, CDCl_3) δ 1.45 (s, 9H), 5.14 (d, 1H, $J = 10.9$ Hz), 5.30 (s, 1H), 5.62 (d, 1H, $J = 17.6$ Hz), 6.66 (dd, 1H, $J_1 = 17.6$ Hz, $J_2 = 11.0$ Hz), 7.16 (d, 1H, $J = 1.8$ Hz), 7.42 (d, 1H, $J = 1.6$ Hz); $^{13}\text{C NMR}$ (125 MHz, CDCl_3) δ 29.5, 35.0, 112.0, 122.5, 126.2, 126.3, 130.2, 136.3, 137.3, 152.0.

2,2'-bisphenoxyphosphorus chloride (7)



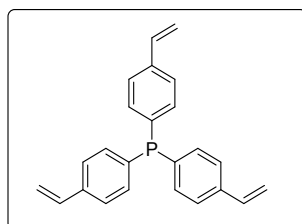
yellow liquid; $^1\text{H NMR}$ (400 MHz, CDCl_3) δ 7.20 (d, 2H, $J = 7.9$ Hz), 7.31 (t, 2H, $J = 7.4$ Hz), 7.37 (td, 2H, $J_1 = 7.7$ Hz, $J_2 = 1.6$ Hz), 7.46 (dd, 2H, $J_1 = 7.5$ Hz, $J_2 = 1.6$ Hz); $^{13}\text{C NMR}$ (100 MHz, CDCl_3) δ 122.2 (d, $J = 1.9$ Hz), 126.2, 129.4, 130.1, 130.9 (d, $J = 3.5$ Hz), 149.2 (d, $J = 5.7$ Hz); $^{31}\text{P NMR}$ (161.8 MHz, CDCl_3) δ 179.4.

6,6'-(3,3'-di-tert-butyl-5,5'-divinylbiphenyl-2,2' diyl)bis(oxy)didibenzo [1,3,2]dioxaphosphepine (A)



a white solid, m.p. 185 °C; $^1\text{H NMR}$ (400 MHz, CDCl_3) δ 1.32 (s, 9H), 5.24 (dd, 1H, $J_1 = 10.9$ Hz, $J_2 = 0.5$ Hz), 5.74 (dd, 1H, $J_1 = 17.6$ Hz, $J_2 = 0.5$ Hz), 6.75 (dd, 1H, $J_1 = 17.6$ Hz, $J_2 = 10.9$ Hz), 6.72 (d, 1H, $J = 7.6$ Hz), 7.01 (td, 1H, $J_1 = 7.9$ Hz, $J_2 = 1.3$ Hz), 7.10-7.15 (m, 2H), 7.23 (td, 1H, $J_1 = 7.5$ Hz, $J_2 = 1.2$ Hz), 7.29 (td, 1H, $J_1 = 7.8$ Hz, $J_2 = 1.8$ Hz), 7.35 (dd, 1H, $J_1 = 7.7$ Hz, $J_2 = 1.6$ Hz), 7.39-7.44 (m, 2H), 7.54 (d, 1H, $J = 2.3$ Hz); $^{13}\text{C NMR}$ (100 MHz, CDCl_3) δ 30.4, 35.3, 113.4, 122.3, 123.1, 124.8, 124.9, 126.1, 128.7, 128.8, 129.4, 129.6, 129.8, 131.2, 131.3, 131.5, 132.5, 136.4, 141.9, 149.0, 149.7, 150.2; $^{31}\text{P NMR}$ (161.8 MHz, CDCl_3) δ 144.5; **HRMS** (ESI):m/z calc. for $\text{C}_{48}\text{H}_{44}\text{O}_6\text{P}_2$ $[\text{M}+\text{H}]^+$:779.2686, found:779.2697.

tris(4-vinphenyl)phosphane (B)



a white solid, m.p. 75 °C; $^1\text{H NMR}$ (400 MHz, CDCl_3) δ 5.26 (d, 1H, $J = 11.1$ Hz), 5.76 (d, 1H, $J = 17.5$ Hz), 6.69 (dd, 1H, $J_1 = 17.6$ Hz, $J_2 = 10.9$ Hz), 7.25-7.29 (m, 2H), 7.35-7.37 (m, 2H); $^{13}\text{C NMR}$ (100 MHz, CDCl_3) δ 114.7, 126.3 (d, 6C, $J = 7.0$ Hz), 133.8 (d, 3C, $J = 19.4$ Hz), 136.3, 136.6 (d, 6C, $J = 10.8$ Hz), 137.9; $^{31}\text{P NMR}$ (161.8 MHz, CDCl_3) δ -6.8;

NMR spectra of compounds 1-7 and A, B

